Prospects of constraining the dense matter equation of state from observations and data analysis of radio pulsars in binaries

Manjari Bagchi

Institute of Mathematical Sciences (IMSc), Chennai, India

September 28, 2017

Why pulsars?

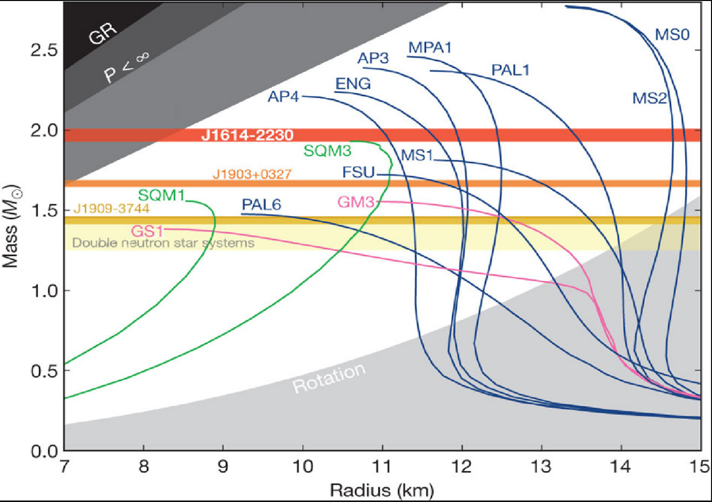

Extra contribution in $\dot{\varpi}$ might be useful to constrain EoS via measurement of $I_{\rm NS}$.

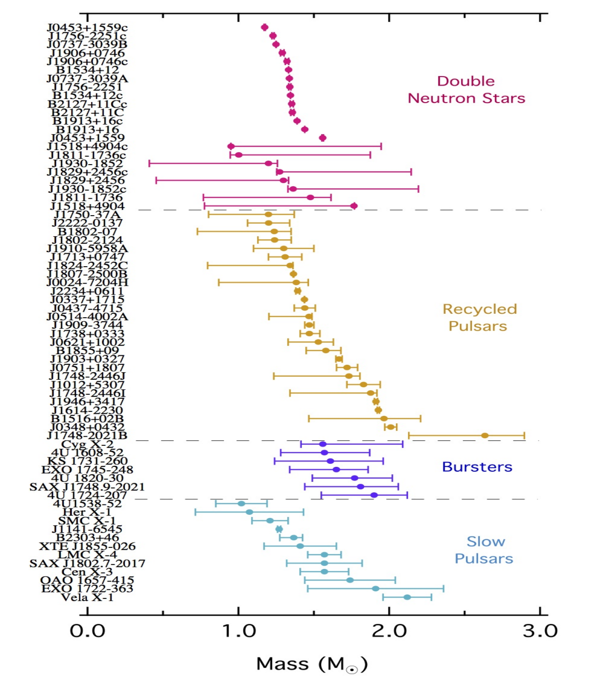
J0453+1559c
J1756-2251c
J0737-3039B
J1906+0746
J1906+0746c
B1534+12
J0737-3039A
J1756-2251
B1534+12c
B2127+11Cc
B2127+11C
B1913+16c
B1913+16
J0453+1559
J1518+4904c
J1811-1736c
J1930-1852
J1829+2456c
J1829+2456
J1930-1852c
J1811-1736
J1518+4904
J1750-37A
J2222-0137
B1802-07
J1802-2124
J1910-5958A
J1713+0747
J1824-2452C
J1807-2500B
J0024-7204H
J2234+0611
J0337+1715
J0437-4715
J0514-4002A
J1909-3744
J1738+0333
J0621+1002
B1855+09
J1903+0327
J0751+1807
J1748-2446J
J1012+5307
J1748-2446I
J1946+3417
J1614-2230
B1516+02B
J0348+0432
J1748-2021B
Cyg X-2
4U 1608-52
KS 1731-260
EXO 1745-248
4U 1820-30
SAX J1748.9-2021
4U 1724-207
4U1538-52
Her X-1
SMC X-1
J1141-6545
B2303+46
XTE J1855-026
LMC X-4
SAX J1802.7-2017
Cen X-3
OAO 1657-415
EXO 1722-363
Vela X-1
Double Neutron Stars
Recycled Pulsars
Bursters
Slow Pulsars
0.0
1.0
2.0
3.0
Mass (M☉)

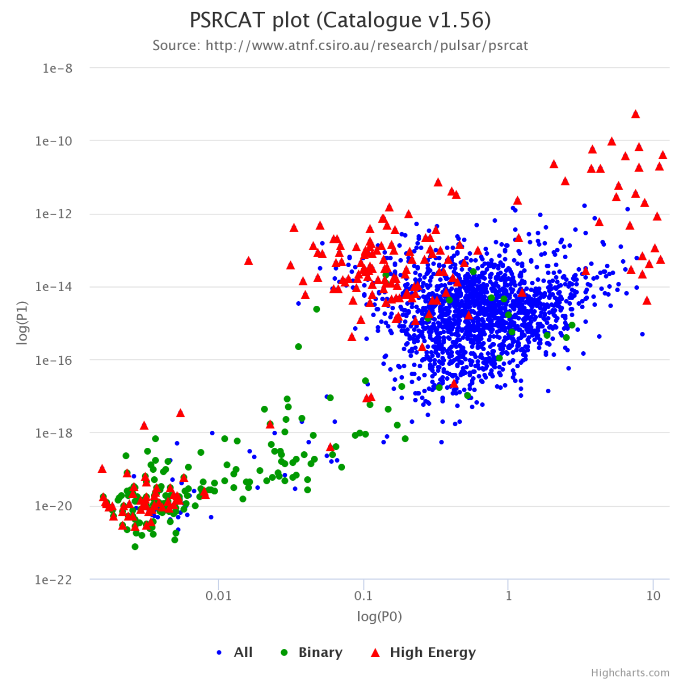

PSRCAT plot (Catalogue v1.56)
Source: http://www.atnf.csiro.au/research/pulsar/psrcat
1e−8
1e−10
1e−12
1e−14
1e−16
1e−18
1e−20
1e−22
log(P1)
0.01
0.1
1
10
log(P0)
All
Binary
High Energy
Highcharts.com

Neutron Stars as Radio Pulsars

(2405)

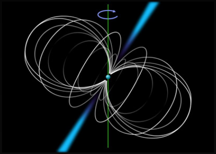

Isolated

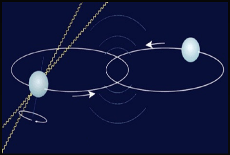

Binary (∼241)

(i) NS-low mass (28)

(ii) NS-MS (∼2)

(iii) NS-WD (∼200)

(iv) NS-NS (11+4)

(v) NS-BH (0)

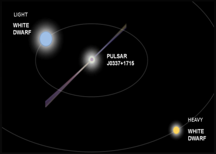

Triple (2)

NS-WD-WD (1)

NS-WD-planet (1)

Rituals of a pulsar astronomer

- Discover a pulsar, confirm it - you know $P_{\rm spin}$, DM, RA, DEC.
- Start to time it - measure/imporve $P_{\rm spin}$, $\dot{P}_{\rm spin}$ DM, RA, DEC.
- Other properties: glitch, null, emission in other wavelength, proper motion, etc.
- Keep on timing (record 'Time of Arrival' of pulses) - you can measure classical (Keplerian) orbital parameters and post-Keplerian parameters (effects of GR).
- Testing theories of gravity, constraining dense matter equation of state, detecting low-frequency gravitational waves, etc.

Pulsar timing in a nutshell

* We measure $t_{i,earth} = t_{i,pulsar} + d_i/c$

- motion of the earth modelled (baycentering), motion of the pulsar remains
- Keplerian orbital parameters: e, P_b, $a_p \sin i$, ϖ
- GR (and other extra) effects are taken care of as PK parameters

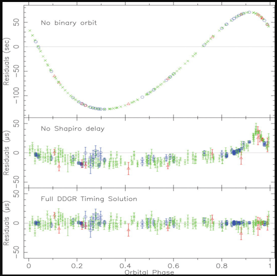

(Science 320 (2008) 1309.)

Some PK parameters

$\varpi \equiv \omega$

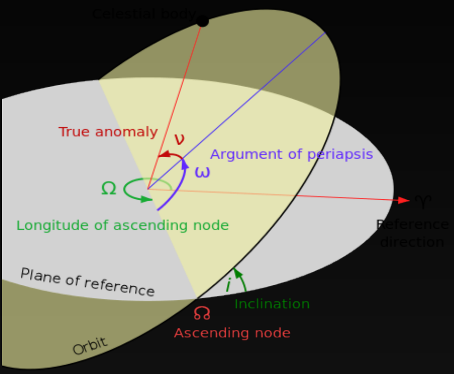

[In some literature $\varpi = \omega + \Omega$]

$\dot{\varpi}$

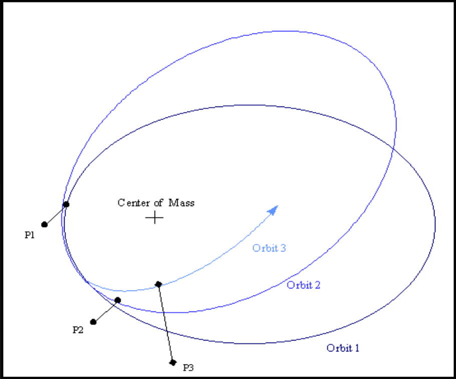

Some PK parameters

$\dot{P}_b$, $\dot{e}$

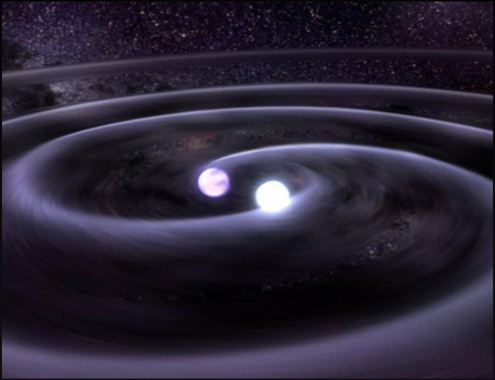

first *indirect* detection of gravitational wave (PSR B1913+16 by Hulse & Taylor, 1975; Nobel prize in 1993)

Some PK parameters

Shapiro Delay:

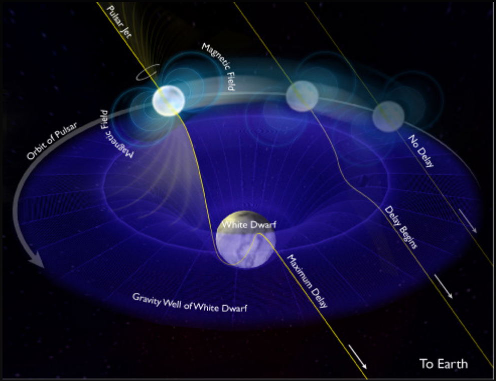

$$s = \sin i,\ r = \frac{Gm_c}{c^3}$$

Some PK parameters

Einstein Delay (γ): general relativistic time dilation

Clocks that are far from massive bodies run more quickly, and clocks close to massive bodies run more slowly.

So there would be a difference between two clocks - one at the pulsar and another on earth (Einstein delay for isolated pulsars) – for a binary pulsar, the clock on the pulsar will be affected by the companion also!

Good timing solution: best match of observed and predicted ToAs.

We get: e, P_b, $a_p \sin i$, ω; $\dot{\varpi}$, $\dot{P}_b$, r, s, γ (fit parameters)

$$\dot{\varpi} = 3T_\odot^{2/3}\left(\frac{P_b}{2\pi}\right)^{-5/3}\frac{1}{1-e^2}(m_p+m_c)^{2/3} \qquad m_c = f1(P_b, e, m_p, \dot{\varpi})$$

$$\gamma = T_\odot^{2/3}\left(\frac{P_b}{2\pi}\right)^{1/3} e\,\frac{m_c(m_p+2m_c)}{(m_p+m_c)^{4/3}} \qquad m_c = f2(P_b, e, m_p, \gamma)$$

$$r = T_\odot m_c \qquad m_c = r/T_\odot$$

$$s = \sin i = T_\odot^{-1/3}\left(\frac{P_b}{2\pi}\right)^{-2/3}\mathcal{X}\,\frac{(m_p+m_c)^{2/3}}{m_c} \qquad m_c = f4(P_b, e, m_p, \mathcal{X}, s)$$

where $\mathcal{X} = \frac{a_p \sin i}{c}$, $P_b^2 = \frac{4\pi^2 a_R^3}{G(m_p+m_c)} = \frac{4\pi^2}{G(m_p+m_c)}\left[\frac{a_p(m_p+m_c)}{m_c}\right]^3$

$$\dot{P}_b = -\frac{192\pi}{5}T_\odot^{5/3}\left(\frac{P_b}{2\pi}\right)^{-5/3} f(e)\frac{m_p m_c}{(m_p+m_c)^{1/3}} \qquad m_c = f5(P_b, e, m_p, \dot{P}_b)$$

$$f(e) = \frac{1+(73/24)e^2+(37/96)e^4}{(1-e^2)^7/2}, \quad T_\odot = \frac{GM_\odot}{c^3} = 4.92540\ \mu\text{s}$$

Use of PK parameters (GR, 1PN)

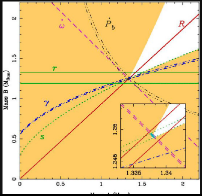

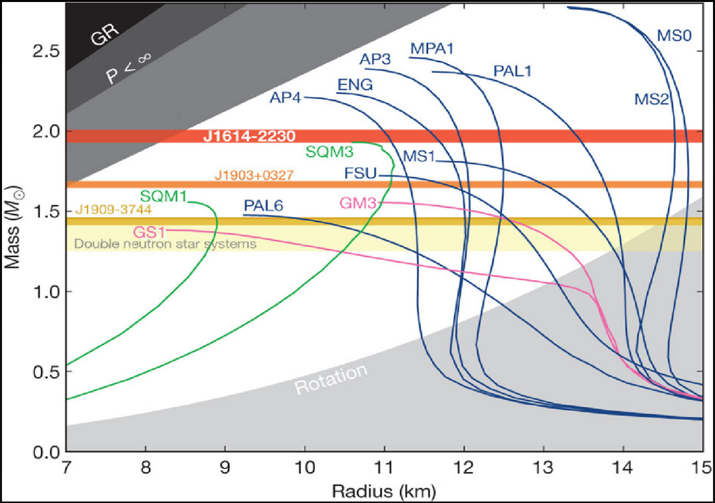
GR
P < ∞
J1614-2230
J1903+0327
J1909-3744
Double neutron star systems
Rotation
SQM1
SQM3
GS1
GM3
PAL6
FSU
MS1
AP4
ENG
AP3
MPA1
PAL1
MS0
MS2
Mass ($M_\odot$)
Radius (km)
0.0
0.5
1.0
1.5
2.0
2.5
7
8
9
10
11
12
13
14
15

Some extra terms in PK parameters

$$\vec{J} = \vec{L} + \vec{S}_1 + \vec{S}_2$$

Precession of the spin

$$\overrightarrow{\Omega}_{\mathrm{S_i}} = \overrightarrow{\Omega}_{\mathrm{PN_i}} + \overrightarrow{\Omega}_{\mathrm{LT_i}} + \overrightarrow{\Omega}_{\mathrm{QS_i}}$$

$$\dot{\hat{S}}_i = \overrightarrow{\Omega}_{\mathrm{S_i}} \times \hat{S}_i$$

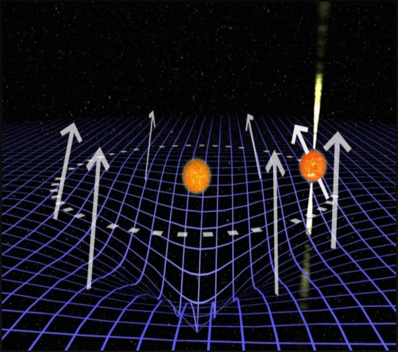

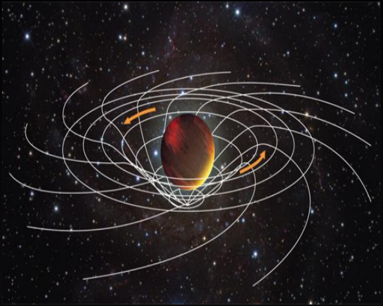

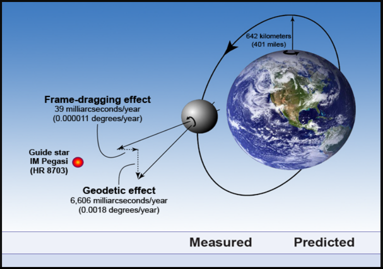

Precession of the spin

Spin Precession of a pulsar can be measured!

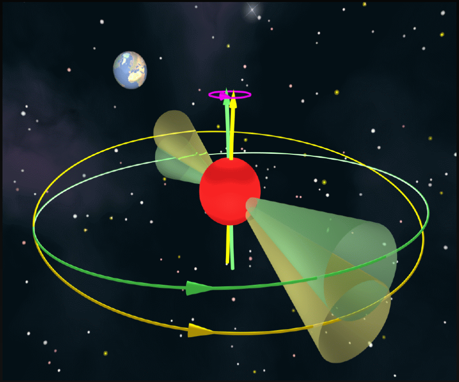

Precesion of the orbit:

Barker and O'Connell (1979) Gen. Rel and Grav.

$$\overrightarrow{\Omega}_{\rm prec} = \overrightarrow{\Omega}_{\rm PN} + \overrightarrow{\Omega}_{\rm LT_1} + \overrightarrow{\Omega}_{\rm LT_2} + \overrightarrow{\Omega}_{\rm Qs_1} + \overrightarrow{\Omega}_{\rm Qs_2} + (\overrightarrow{\Omega}_{\rm Qt_1} + \overrightarrow{\Omega}_{\rm Qt_2})$$

$$\dot{\vec{L}} = \vec{\Omega}_{\rm prec} \times \vec{L}$$

$$\dot{\vec{A}} = \vec{\Omega}_{\rm prec} \times \vec{A} \; (\vec{A} = \vec{p} \times \vec{L} - \mu k \hat{r})$$

$$\vec{\Omega}_{\rm PN} = \Omega^{*}_{\rm PN} \, \widehat{L} = (\Omega^{*}_{\rm 1PN} + \Omega^{*}_{\rm 2PN} + \ldots) \, \widehat{L}$$

$$\vec{\Omega}_{{\rm LT},i} = \Omega^{*}_{{\rm LT},i} \, [3(\widehat{L}.\widehat{S}_i)\widehat{L} - \widehat{S}_i]$$

$$\vec{\Omega}_{{\rm Qs},i} = \Omega^{*}_{{\rm Qs},i} \, [\{5(\widehat{L}.\widehat{S}_i)^2 - 1\}.\widehat{L} - 2(\widehat{L}.\widehat{S}_i).\widehat{S}_i]$$

Precesion of the orbit:

$$\Omega^*_{\rm 1PN} = \frac{3\,T_\odot^{2/3}\,\omega_b^{5/3}}{1-e^2}\,(M_1+M_2)^{2/3}$$

$$\Omega^*_{\rm 2PN} = \frac{3\,T_\odot^{4/3}\,\omega_b^{7/3}}{1-e^2}\,(M_1+M_2)^{4/3}\,f_{0j}$$

$$\Omega^*_{{\rm LT},i} = -\frac{\chi_i\,T_\odot \omega_b^2}{(1-e^2)^{3/2}}\,\frac{M_i(3M_{3-i}+4M_i)}{2(M_1+M_2)}$$

$$\Omega^*_{{\rm Qs},i} = -\frac{q_{s\,i}\,T_\odot^{4/3}\,\omega_b^{7/3}}{(1-e^2)^2}\,\frac{3M_i^2}{4(M_1+M_2)^{2/3}}$$

$\chi_i = \frac{c}{G}\frac{S_i}{M_i^2}$; for star: $S_i = I_i \omega_{s\,i}$; For BH: $\chi \leq 1$ &, $q_s = -\chi^2$ (Thorne 1980)

$\frac{2\pi}{P_{\rm orb}} = \omega_b$, $q_{s\,i} = \frac{c^4}{G^2}\frac{Qs_i}{M_i^3} = \frac{c^4}{G^2}\frac{I_i - I_{3i}}{M_i^3}$

$f_{0j} = \frac{1}{1-e^2}\left(\frac{39}{4}x_j^2 + \frac{27}{4}x_{3-j}^2 + 15 x_j x_{3-j}\right) - \left(\frac{13}{4}x_j^2 + \frac{1}{4}x_{3-j}^2 + \frac{13}{3}x_j x_{3-j}\right)$

$x_j = M_j/(M1 + M_2)$, M_j is being observed. i get summed over, but j is only the psr.

Precesion of the orbit:

For $\widehat{L} \parallel \widehat{S}_i$:

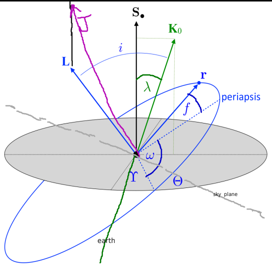

$$\vec{\Omega}_{\rm 1PN} = \frac{3\,T_\odot^{2/3}}{1-e^2}\,\omega_b^{5/3}\,(M_1+M_2)^{2/3}\,\widehat{L} \quad \text{(conventional)}$$

$$\vec{\Omega}_{\rm 2PN} = \frac{3\,T_\odot^{4/3}\,\omega_b^{7/3}}{1-e^2}\,(M_1+M_2)^{4/3}\,f_{0j}\,\widehat{L}$$

$$\vec{\Omega}_{{\rm Qs},i} = -\frac{q_{s\,i}\,T_\odot^{4/3}}{(1-e^2)^2}\,\omega_b^{7/3}\,\frac{3M_i^2}{2(M_1+M_2)^{2/3}}\,\widehat{L}$$

$$\vec{\Omega}_{{\rm LT},i} = -\frac{\chi_i\,T_\odot}{(1-e^2)^{3/2}}\,\omega_b^2\,\frac{M_i(3M_{3-i}+4M_i)}{(M_1+M_2)}\,\widehat{L}$$

Precesion of the orbit ($\widehat{L} \nparallel \widehat{S}_i$):

Damour & Schäfer, 1988, N. Cim. B, 101, 127; $\vec{\Omega}_{\rm prec} = \frac{d\Omega}{dt}\widehat{K}_0 + \frac{d\varpi}{dt}\widehat{L} + \frac{di}{dt}\widehat{\Upsilon}$

$$\dot{\varpi}_{\rm LT} = -\frac{3\beta_0^3\ \omega_b}{1-e^2}\left[g_{s1}\beta_{s1} + g_{s2}\beta_{s2}\right]$$

$$\beta_{sj} = \chi_j = \frac{cI_j\,\omega_{sj}}{Gm_j^2} \qquad \beta_0 = \frac{[G(M_1+M_2)\,\omega_b]^{1/3}}{c} \qquad x_j = \frac{M_j}{M_1+M_2}$$

$$g_{sj} = \frac{x_j\,(4x_j + 3x_{3-j})}{6(1-e^2)^{1/2}} \times \left[\frac{(3\,\sin^2 i - 1)\ \widehat{L}\ + \cos i\ \widehat{K}_0}{\sin^2 i}\right] \cdot \widehat{s}_j$$

For $\widehat{s}_j \parallel [(3\,\sin^2 i - 1)\ \widehat{L} + \cos\ i\ \widehat{K}_0]$:

$$g_{sj,\ max} = \left[3 + \frac{1}{\sin^2\ i}\right]^{1/2} \frac{x_j\,(4x_j + 3x_{3-j})}{6(1-e^2)^{1/2}}$$

For $\widehat{s}_j \parallel \widehat{L}$:

$$g_{sj,\ \parallel} = \frac{x_j\,(4x_j + 3x_{3-j})}{3(1-e^2)^{1/2}} \qquad \text{(matches with Barker} - \text{O'Connell)}$$

difference: $\frac{1}{2}\left[3 + \frac{1}{\sin^2\ i}\right]^{1/2} \in [1.7, 1.0]$ for $i \in [20^\circ, 90^\circ]$.

$$g_{sj} = 0 \text{ if } \widehat{s}_j \perp [(3\,\sin^2 i - 1)\ \widehat{L} + \cos\ i\ \widehat{K}_0]$$

Mesuring $\dot{\varpi}_{\rm LT}$ can lead to measurement of $I_{\rm NS}$ (present in $\beta_{\rm NS}$), which will eventually help to constrain EoS.

NS-NS binaries are the best!

$\dot{\varpi}_{\rm Q}$

Why NS-WD (or NS-MS)systems are not good for $I_{\rm NS}$ determination (one reason):

For $\widehat{L}||\widehat{S}_j$

$$\dot{\varpi}_{\rm Qt,j} = \frac{30\pi}{P_{\rm orb}} \left(\frac{R_c}{a_R}\right)^5 \frac{M_{3-j}}{M_j} \frac{(1+\frac{3}{2}e^2+\frac{1}{8}e^4)}{(1-e^2)^5}$$

where j is the j-th object.

$$\dot{\varpi}_{\rm Qs,j} = \frac{2\pi}{P_{\rm orb}} \left(\frac{R_c}{a_R}\right)^5 \frac{M_{3-j}+M_j}{M_j} \frac{P_{\rm orb}^2}{P_{\rm s,j}^2} \frac{k}{(1-e^2)^2}$$

$Q_{sj} = \frac{G^2 M_j^3}{c^4} q_{sj} = \frac{2}{3G}\, k\, R_j^5\, \omega_{sj}^2$ (Lai, Bildsten, Kaspi, 1995, ApJ)

$R_{ns} \simeq 10$ km, $R_{wd} \simeq (7-14)\times 10^5$ km; $(R_{ns}/R_{wd})^5 = 10^{-16}$

Difficult to know $P_{s,wd}$, R_{wd}, k .. and the isolate Q_{sj} from LT.

Other reasons (i) NS-WD systems are less eccentric so difficult to identify the periastron and measure $\dot{\varpi}$, (ii) Longer P_b, smaller e

$\widehat{L}||\widehat{S}_j$ makes life simpler :)

NS-NS binaries in globular clusters are useless for $I_{\rm NS}$ mesurement, as they can be dynamically formed.

$I_{\rm NS}(M_{NS}$, **EoS**, $P_{s,NS})$:

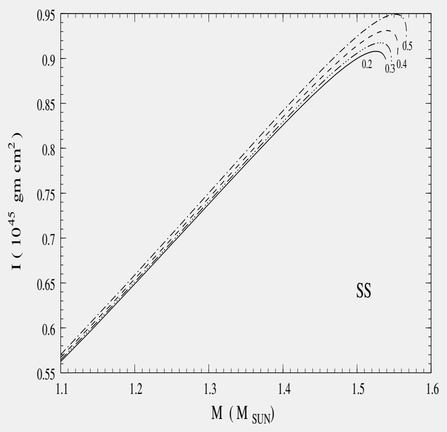

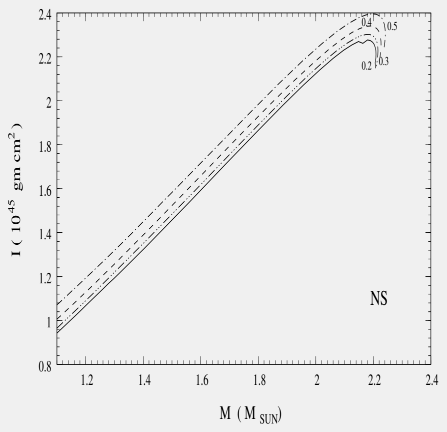

Bagchi, 2010, New Astronomy, 15, 126

Ω in units of 10^4 s^{-1} (for the fastest pulsar $\Omega = 0.45 \times 10^4$ s^{-1})

Rapidly **R**otating **N**eutron **S**tar Code: http://www.gravity.phys.uwm.edu/rns/

$I_{\rm NS}(M_{NS}$, EoS, $P_{s,NS})$:

$P_{\rm spin,A} = 0.022699$ s

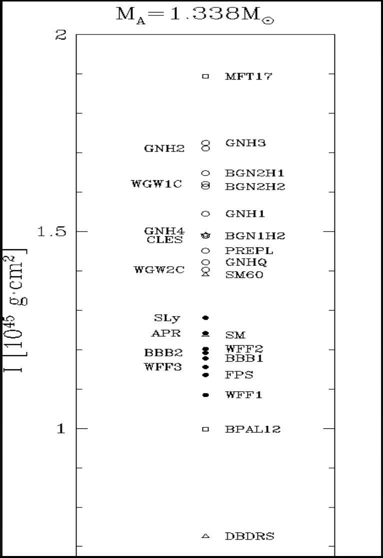

Bejger, Bulik, Haensel, 2005, MNRAS, 364, 635

Estimation of $I_{\rm NS}$ of a pulsar

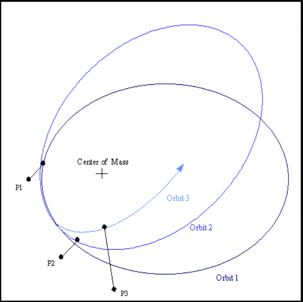

1) $\dot\varpi$ should be large enough, so easy to measure and error is small.

2) $\dot\varpi_{LT,p}$ should be $\gg \dot\varpi_{LT,c}$ OR both known (satisfied fo PSR J0737-3039A/B)

3) $\dot\varpi_{LT,psr}$ should be $\gtrsim$ than the error in the observed value of $\dot\varpi$

Best estimate of $\dot\varpi$ (PSR J0737-3039A/B): $16.89947 \pm 0.00068\ \mathrm{deg\ yr}^{-1}$

$\frac{\dot\varpi_{\rm 2PN}}{\dot\varpi_{\rm 1PN}} \sim 10^{-5}$ $\frac{\dot\varpi_{\rm LT\|,tot}}{\dot\varpi_{\rm 1PN}} \sim 10^{-6}$ $(I_{NS} = 10^{45}\ \mathrm{g\ cm}^2)$

$e = 0.0878,\ P_b = 0.1023$ days

- PSR J0737-3039A/B is being timed
- Discovery of even a better system (higher e, shorter P_b) will be great
- Search for new pulsars
- Many ongoing pulsar surveys
- Arecibo drift-scan, uGMRT pilot survey (just started)

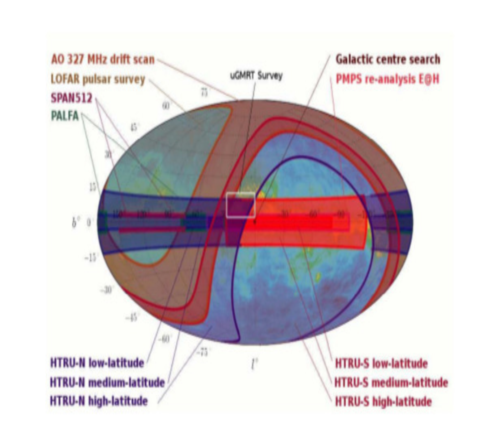

https://www.mpifr-bonn.mpg.de/research/fundamental/pulsarsurveys

- PSR J0737-3039A/B is being timed
- Discovery of even a better system (higher e, shorter P_b) will be great
- Search for new pulsars
- Many ongoing pulsar surveys
- Arecibo drift-scan, uGMRT pilot survey (just started)

AO327: * 8 MSPs (binaries), 7 slow pulsars and 11 RRATs.

** One slow pulsar was found in the data taken during the observatory shut-down for hurricane Isaac in 2012.

*** Two MSPs are included in the NANOGrav set.

**** NS-NS with most asymmetric mass ratio (PSR J0453+1559; 2015, ApJ, 812, 143): $M_p = 1.559 \pm 0.005\ \mathrm{M}_\odot, \quad M_c = 1.174 \pm 0.004\ \mathrm{M}_\odot$

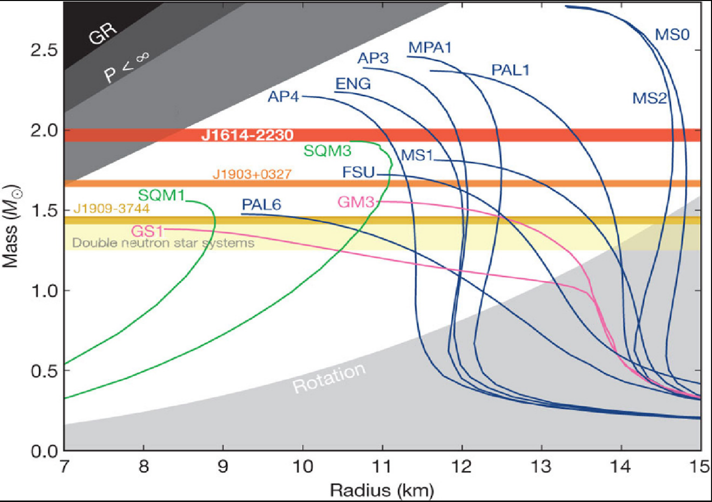

Rotationally excluded region is for the fastest psr Ter5ad (716 Hz; 1.39 ms)

$M_p \sim 2.5\ \mathrm{M}_\odot$

$M_p \sim 1\ \mathrm{M}_\odot$, $P_s \sim 1$ ms

SKA:

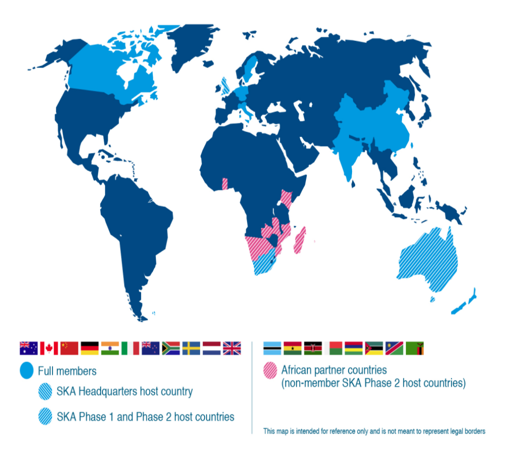

1) mid (0.350–5 GHz) and high (5–14 (45) GHz) frequency antennas in South Africa

2) low-frequency (0.050–0.350 GHz) antennas in Australia.

uGMRT as SKA pathfinder:

30 antennas each of 45 metre diameter

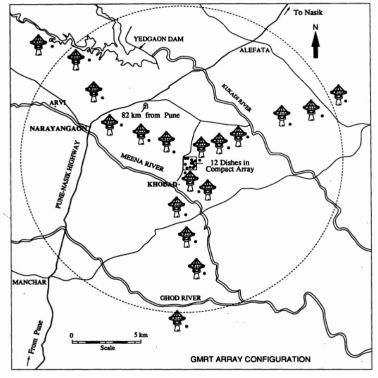

uGMRT as SKA pathfinder:

30 antennas each of 45 metre diameter

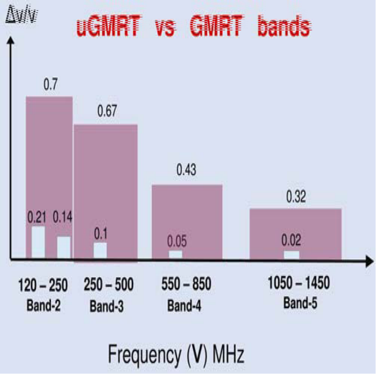

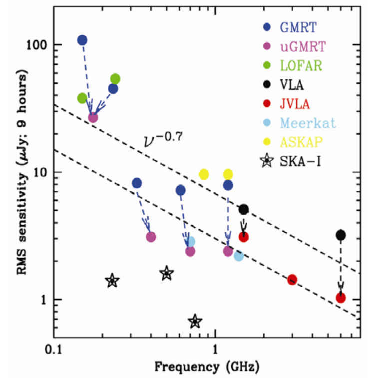

Current Science, 2017, Volume 113, No 4.

** Real time transient detection pipeline in progress **

Neutron stars in X-ray: ASTROSAT

ASTROSAT | astrosat - Google Chrome

Not secure | astrosat.iucaa.in

Password *

Request new password

Log in

News

08 Dec 2015:
LAXPC First Light Report

04 Dec 2015:
UVIT First Light

01 Dec 2015:
Sky images obtained in all three UVIT channels (FUV, NUV, VIS). Performance is normal.

30 Nov 2015:
Doors of both the UV Imaging telescopes opened successfully

03 Nov 2015:
SXT First Light Report

27 Oct 2015:
SXT made operational on Oct 26. First light image of Blazar PKS2155-304 obtained. Performance normal. Calibrations underway.

SPIE 2014 paper on Astrosat

Astrosat Outreach Booklet

ASTROSAT is a multi-wavelength astronomy mission on an IRS-class satellite in a 650-km, near-equatorial orbit. It was launched by the Indian launch vehicle PSLV from Satish Dhawan Space Centre, Sriharikota on **September 28, 2015**. The expected operating life time of the satellite will be more than five years.

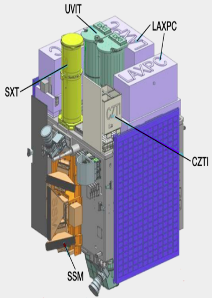

On board ASTROSAT are five astronomy payloads for simultaneous multi-band observations:

- Twin 38-cm Ultraviolet Imaging Telescopes (UVIT) covering Far-UV to optical bands.
- Three units of Large Area Xenon Proportional Counters (LAXPC) covering medium energy X-rays from 3 to 80 keV with an effective area of 8000 sq.cm. at 10 keV.
- A Soft X-ray Telescope (SXT) with conical foil mirrors and X-ray CCD detector, covering the energy range 0.3-8 keV. The effective area will be about 120 sq.cm. at 1 keV.
- A Cadmium-Zinc-Telluride coded-mask imager (CZTI), covering hard X-rays from 10 to 150 keV, with about 6 deg field of view and 480 sq.cm. effective area.
- A Scanning Sky Monitor (SSM) consisting of three one-dimensional position-sensitive proportional counters with coded masks. The assembly is placed on a rotating platform to scan the available sky once every six hours in order to locate transient X-ray sources.

Neutron stars in X-ray: ASTROSAT

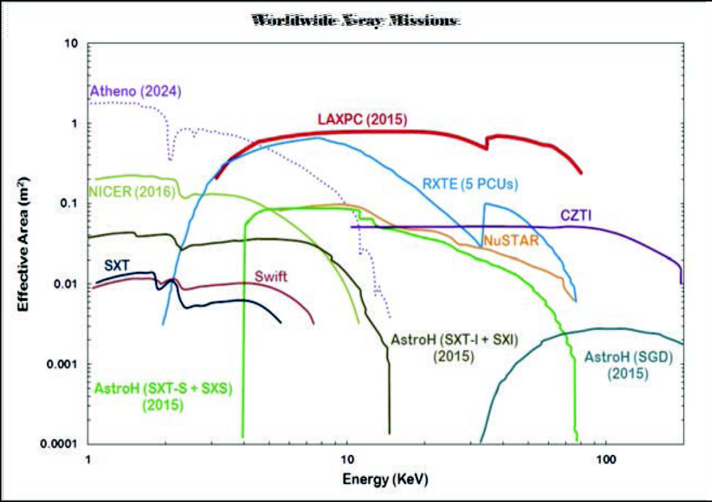

Summary:

- Pulsars are awesome!
- Come to India in 2020. Co-organiser Prashanth Jaikumar ex-faculty of IMSc.
- IMSc ... moderate size QCD group, small astrophysics group,
- Researchers in other institutes including some LIGO people interested in EoS.
- Thank you all ..
- Special thanks to David Blaschke